The phase transition in 2-methyl-1,3-cyclohexanedione crystal

1995 J. Phys.: Condens. Matter 7 7489

(http://iopscience.iop.org/0953-8984/7/38/008)

J. Phys.: Condens. Matter 7 (1995) 7489–7500. Printed in the UK

The phase transition in 2-methyl-1,3-cyclohexanedione crystal

J Wąsicki†, P Czarnecki†, A Katrusiak‡, C Ecolivet§ and M Bertault§

† Institute of Physics, A Mickiewicz University, 61-614 Poznań, Poland

‡ Institute of Chemistry, A Mickiewicz University, 60-780 Poznań, Poland

§ Groupe Matière Condensée et Matériaux, Université de Rennes I, 35042 Rennes, France

Received 27 March 1995, in final form 18 May 1995

Abstract. The phase transition in 2-methyl-1,3-cyclohexanedione crystal was investigated by Brillouin scattering, nuclear magnetic resonance (NMR), calorimetry and dielectric permittivity measurements. Thermal anomalies related to the second-order phase transition were observed at $T_c = 243$ K. The transition entropy was found to be $\Delta S = 5.7$ J mol^{-1} K^{-1}. NMR results are interpreted assuming two models of molecular reorientation, whereas dielectric studies indicate an activation process around T_c. The elastic constants measured in the Brillouin scattering experiment have been related to the structure; its temperature dependence confirms that the phase transition has slow dynamics like in an order–disorder transformation without any softening of modes. Considerable differences can be noted between the phase transitions and molecular dynamics in the crystals of 2-methyl-1,3-cyclohexanedione and the analogous 1,3-cyclohexanedione.

1. Introduction

Recently crystal structures and solid-state phase transitions have been studied in the series of simple cyclic β-diketoalkanes [1–4]. All these substances are present in the enolized form in the crystalline state, and the molecules are linked by strong hydrogen bonds into chains. One of these molecules, 1,3-cyclohexanedione (CHD), was found to undergo an interesting phase transition at 289 K, which visibly changes the crystal shape. The CHD crystals are monoclinic, space group $P2_1/c$, and this symmetry does not change at the phase transition [2]. The structural phase transition in CHD is driven by ordering of the $C(5)H_2$ methylene group and the transfer of the enolic proton between donor and acceptor sites in the hydrogen bond. The molecular structure of 2-methyl-1,3-cyclohexanedione (hereafter MCHD) resembles that of CHD in many aspects, as it contains only one additional methyl group substituted at carbon atom C(2) (figure 1). Thus it contains a six-membered ring which is puckered, and its C(5) atom moves from one side of the ring plane to the other. The molecule can also transform in such a way that the enolic proton changes its position in the hydrogen bonds. The MCHD molecules also form similar chains connected by hydrogen bonds (figure 2). Recent structural studies [1] showed that the crystals are orthorhombic, space group *Ibam*. At room temperature the $C(5)H_2$ and $C(4)H_2$ methylene groups are disordered and the molecular ring in this compound presents a half-chair conformation. In the CHD structure, the hydrogen-bonded planar chains lie in crystallographic general positions, whereas in the MCHD structure they lie on mirror planes and an onset of ordering must change the symmetry of the crystal.

0953-8984/95/387489+12$19.50

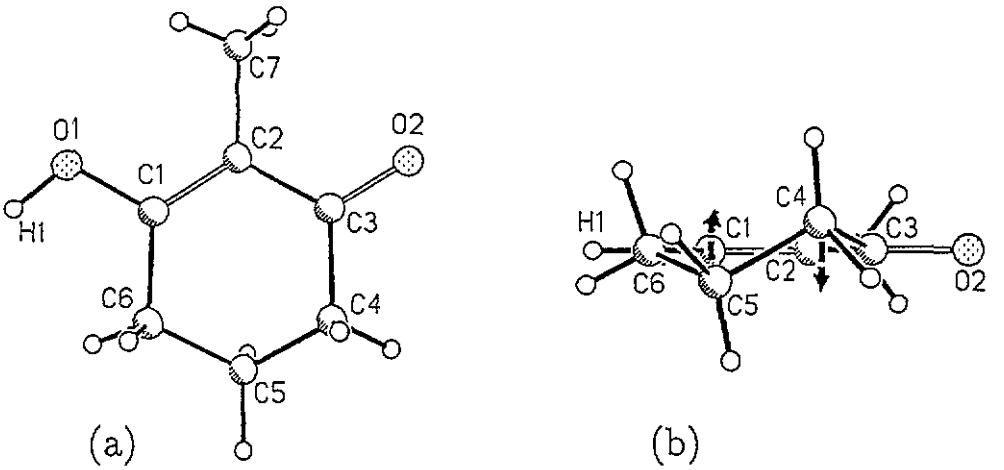

Figure 1. 2-Methyl-1,3-cyclohexanedione molecule viewed (*a*) perpendicular to the molecular ring and (*b*) along the direction lying in the plane of molecular ring and perpendicular to the C(4)–C(5) bond. The double bonds are shown as open lines. The arrows indicate trajectories of large-amplitude vibrations of methylene groups $C(4)H_2$ and $C(5)H_2$.

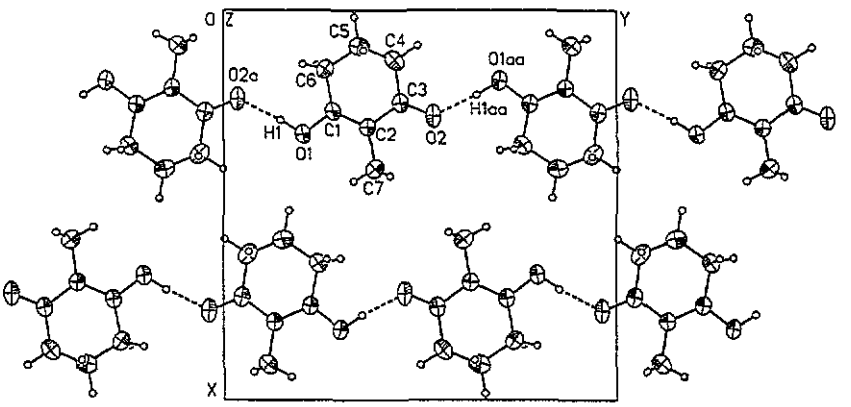

Figure 2. Crystal structure of MCHD at room temperature viewed down **c**.

In both CHD and MCHD structures disorder is caused by large-amplitude intramolecular vibrations. Originally it was assumed that the ring transformations take place only above T_c. However recent NMR studies of molecular dynamics [4] showed that strong molecular rearrangements are present both in the ordered as well as in the disordered crystalline phases of CHD.

The main aim of this paper is to investigate the physical properties of the MCHD crystals in order to compare phase transitions in MCHD and CHD. Several experimental techniques have been applied. The NMR studies allowed us to estimate the activation energy and molecular reorientation of MCHD crystal. There were speculations in [1] about the crystal symmetry of MCHD in the low-temperature phase, which could belong to the *Iba*2 symmetry or to a monoclinic symmetry. In the case of *Iba*2 symmetry the phase transition could be ferroelectric, whereas in the case of monoclinic symmetry the phase transition could be ferroelastic. Dielectric and Brillouin scattering experiments give us

additional information about possible ferroelectric or ferroelastic type of phase transition. The Brillouin scattering experiment allowed us also to obtain the elastic constants of MCHD at room temperature and relate them to the molecular arrangements in the crystal structure.

2. Experimental details

Calorimetric measurements were carried out by differential scanning calorimetry (DSC) using a Perkin-Elmer DSC-7 calorimeter in the temperature range 150–300 K on polycrystalline samples. The heating rate was 10 K min^{-1} and the weight of the sample was 28.840 mg.

Single crystals of MCHD were obtained by slow evaporation of acetone solution; they were colourless prisms with typical dimensions $1.5 \times 1 \times 0.2$ mm^3.

The dielectric permittivity was measured on a single-crystal sample by an Impedance Analyser HP-4192A. The dimensions of the single crystal we used were $3 \times 0.5 \times 0.2$ mm^3, and silver electrodes were deposited on its (010) and $(0\bar{1}0)$ surfaces. Dielectric measurements were performed at frequencies between 10 kHz and 13 MHz in the temperature range 77–330 K. The measured capacitance of the sample was about 1 pF at room temperature. The small size of the obtained single crystals did not allow us to measure dielectric permittivity in other crystallographic directions.

For NMR measurements the polycrystalline sample of MCHD was outgassed by the freeze–pump–thaw technique and sealed under vacuum in a glass ampoule.

Measurements of NMR second moment M_2 were carried out, using a wide-line spectrometer operating at a Larmor frequency of 28 MHz. The second-moment values were calculated by numerical integration of the absorption curve derivatives and corrected for the finite modulation amplitude.

Measurements of spin–lattice relaxation times T_1 were performed using pulse spectrometers operating at 25 and 60 MHz by saturation recovery pulse sequence.

The temperature of the sample was controlled by means of a gas-flow cryostat and monitored with a Pt resistor to an accuracy of 1 K for both wide-line and pulse spectrometers.

Measurements of NMR second moments were carried out between 110 and 423 K.

Measurements of T_1 were performed from 95 to 453 K and from 74 to 345 K for 60 and 25 MHz respectively.

The Brillouin scattering spectrometer (located in Rennes) is a tandem of Fabry–Perot interferometers designed by Sandercock with a set-up similar to the one reported in [5] except that in order to minimize the length of the optical path each Fabry–Perot is individually triple-passed. The resulting finesse is about 70 and the contrast is estimated to be about 10^{12}. Backscattering experiments along the b direction have been performed between 200 K and 300 K.

3. Results and discussion

3.1. Brillouin scattering

Room-temperature experiments have been performed using either back- or right-angle scattering. Due to the small size of samples we have not been able to determine the absolute value of the refractive indices, but with different backscattering configurations we can reliably obtain the ratios of refractive indices. In order to estimate elastic constants we have assumed a plausible value for the lowest refractive index as $n_c = 1.5$; hence $n_a = 1.61$ and $n_b = 1.96$. The birefrigence is rather large for a single-ring molecule, which probably

follows from the fact that two oxygen atoms are aligned nearly along the largest value, which is the b direction. Elastic wave propagation is also found to be highly anisotropic since a very high value for organic crystals of 6300 m s^{-1} is found along the b axis whereas the lowest longitudinal velocity is found along (a, c) bisector with 2595 m s^{-1} (figure 3). Although these values are based on a hypothetical value of $n_c = 1.5$, it is very likely that they are correct to $\pm 10\%$, which still gives a large velocity along the b axis and a large elastic anisotropy. The origin of elastic anisotropy is almost obvious since oxygen atoms evenly distributed along the b axis are involved in strong hydrogen bonds approximately along this direction. By assuming a chain-like model for elastic wave propagation one finds for the different directions a force constant $k_c = 5.4$ N m^{-1} which is typical of van der Waals interactions in organic crystals. A much higher value is found along the b axis with $k_b = 18$ N m^{-1} and an intermediate one along a, $k_a = 12$ N m^{-1}, probably because of some contribution of the hydrogen bonds. The elastic constants of MCHD are collected in table 1. It should be kept in mind that the true values, once n_c is known, will be obtained by multiplication by a factor $0.444 n_c^2$. Experimental errors estimated on all experiments in different scattering geometries should also be equally corrected.

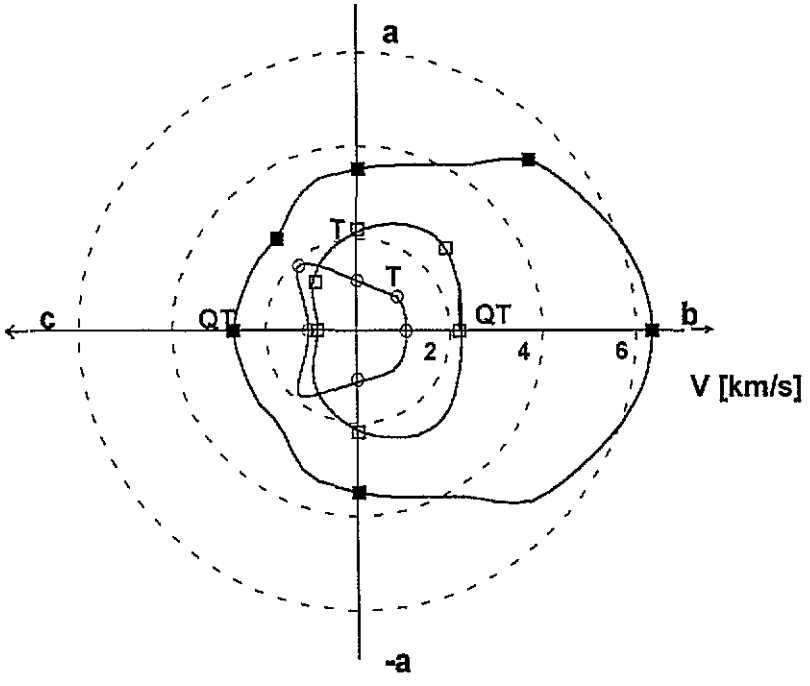

Figure 3. Sound velocity diagram in the (a, b) (right) and (a, c) planes (left) at room temperature. The outer curve corresponds to the quasilongitudinal mode whereas the labelled 'T' and 'QT' correspond respectively to true transverse waves polarized perpendicular to the propagation plane and quasitransverse waves polarized in the propagation plane. The maximum longitudinal velocity (6.3 km s^{-1}) corresponds to the OY axis of figure 2.

Backscattering experiments along the b axis, which is the direction of hydrogen bond chains, do not reveal any compression-related anomaly between 300 K and 200 K, whereas the transverse mode polarized along the c axis ($V_t = (C_{44}/\rho)^{1/2}$) exhibits a change of slope by a factor of 2 around 246 ± 2 K. This is an indication of the phase transition reported by Katrusiak [1] at 244 ± 1 K and assigned to an ordering of methylene groups

Table 1. Elastic constants C_{ij} of MCHD (GPa).

14.9 ± 0.3	11.1 ± 1	3.26 ± 0.8			
11.1 ± 1	50.0 ± 0.1	$(\cong -C_{44})$			
3.26 ± 0.8	$(\cong -C_{44})$	9.1 ± 0.25			
			1.15 ± 0.05		
				1.65 ± 0.15	
					6.43 ± 0.2

in the molecular ring. The anomaly observed is characteristic of a biquadratic coupling between the order parameter and the e_4 strain; the change of slope in the low-temperature phase is a contribution of the square of the order parameter to the elastic constant C_{44}. No dispersion-like or softening anomaly has been observed.

Our observation of the temperature dependence of the Brillouin frequency shifts versus temperature does not exhibit any step and so agrees with the previous study which states that the structural phase transition is continuous.

3.2. Calorimetric measurements

The temperature dependence of the specific heat of the MCHD crystal is shown in figure 4. The thermal anomaly has a long tail below the transition point estimated at $T_c = 243$ K. The shape of the $C_p(T)$ dependence as well as the lack of temperature hysteresis indicate that the phase transition confirms its continuous character. We calculated the anomalous part of the molar entropy variation of the phase transition from the following relation:

$$\Delta S = \int [C_p(T) - C_p^b(T)]/T \, dT \tag{1}$$

where $C_p^b(T)$ stands for the nonlinear baseline extrapolated from the measurement points far from T_c.

The result of the integration is shown in figure 4. The increase of entropy associated with the phase transition is 5.7 J mol^{-1} K^{-1}, which is practically equal to the value $R \ln 2$ and confirms the typical order–disorder type of the phase transition.

The disorder in MCHD above T_c is caused by the C(4) and C(5) methylene groups [1]. The molecule of MCHD lies in the mirror plane and only the disordered methylene carbons C(4) and C(5) lie out of this plane at two non-equivalent positions (figure 1(*b*)). The structural phase transition induces the ordering of C(4) and C(5) below T_c and therefore the anomalous change of entropy is expected to be equal to $R \ln 2$.

3.3. NMR measurements

The temperature dependence of the second moment (M_2) is shown in figure 5. The second moment observed at low temperatures (17 G^2) decreases gradually between 120 K and 223 K to the value of 15.3 G^2. Above 223 K, M_2 decreases rapidly to the value of 10 G^2 observed at 250 K. Then up to about 350 K, M_2 has a constant value. At higher temperatures second moments start to decrease to the value 8 G^2 observed at 423 K. Close to the temperature of the phase transition (244 K) only a small discontinuity of M_2 is observed.

The temperature variations of the spin–lattice relaxation times T_1 are shown in figure 6. Spin–lattice relaxation times measured at 60 and 25 MHz show minima of 104 ms at 326 K and 43 ms at 300 K, respectively. Below 172 K, T_1 diminishes to 5.49 s observed at 74 K.

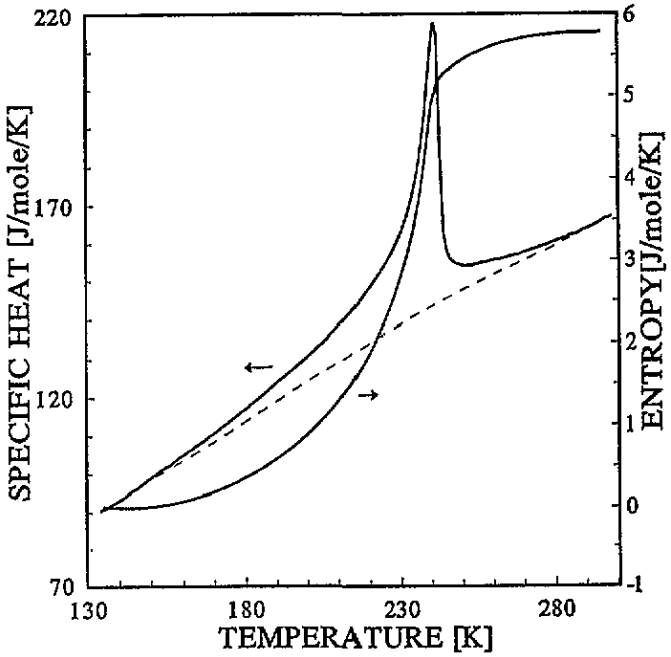

Figure 4. The heat capacity C_p and the entropy change of MCHD obtained from DSC measurements.

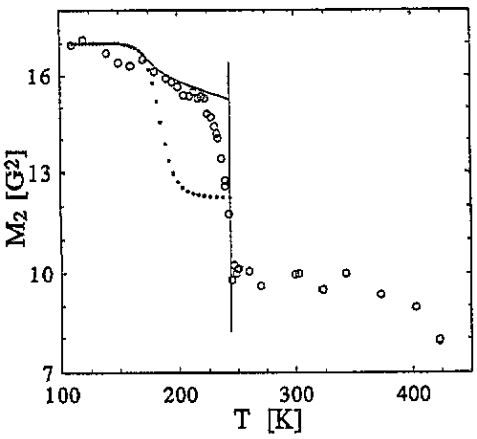

Figure 5. Temperature dependence of the experimental (O) and theoretically calculated second moments: for equivalent barriers (model I) (dotted line) and for inequivalent barriers (model II) (solid line).

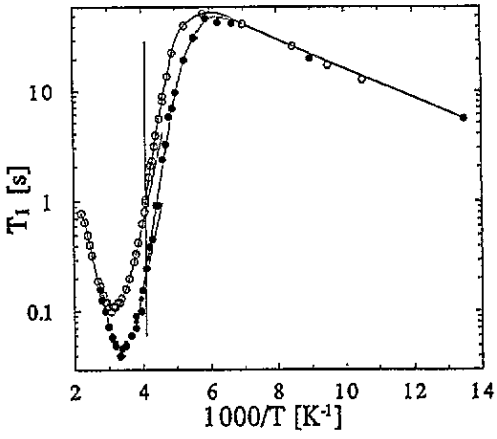

Figure 6. Temperature dependence of the spin–lattice relaxation time T_1 at 60 MHz (O) and 25 MHz (●). The solid lines are theoretical fits to the experimental data.

Magnetization is monoexponential at all temperatures studied. At the temperature of the phase transition, no discontinuity of T_1 is observed.

In order to describe the nature of motions occurring in MCHD the measured values of

the second moment must be compared with the theoretical ones. Using x-ray data reported for MCHD at room temperature [1] we can calculate theoretical second-moment values for a rigid lattice and for models of possible molecular motions. But since an x-ray study does not reveal precise hydrogen atom position in a crystal lattice, we have assumed the C–H bond length to be longer than the one determined from x-ray measurements in order to obtain H–H distance equal to 1.78 Å for CH_3 and CH_2 groups. The theoretical second-moment values were found numerically using the Van Vleck formula [6]. The values calculated for rigid lattice structure and for reorientations of the methyl groups about their C–C bonds are given in table 2.

Table 2. The calculated second moments (G^2).

Type of orientation	M_2^{intra}	M_2^{inter}	M_2^{total}
rigid structure	17.7	6.4	24.1
methyl group	12.3	4.6	16.9

The experimental second-moment values at lower temperatures are in agreement with M_2 estimated for the model of methyl group reorientation about their C_3 symmetry axis.

3.3.1. High-temperature phase. The relaxation rate for protons of MCHD can be expressed as:

$$1/T_1 = \tfrac{3}{10}(1/T_1)^{CH_3} + \tfrac{6}{10}(1/T_1)^{RP} + \tfrac{1}{10}(1/T_1)^{H} \tag{2}$$

where the first term describes the relaxation rate of methyl group reorientation, the second one describes conformational motion of the methylene group in the cyclohexene ring (ring puckering) and the third one describes proton motion along the hydrogen bond. The fact that the ratio of both T_1 minima ($104/43 = 2.4$) is equal to the respective resonance frequencies indicates that the motion in the high-temperature phase takes place between symmetric potential wells.

The second term from (2) can be expressed as [7]:

$$(1/T_1)^{RP} = C[\tau_c/(1 + \omega_0^2\tau_c^2) + 4\tau_c/(1 + 4\omega_0^2\tau_c^2)] \tag{3}$$

and

$$C = \tfrac{2}{3}\gamma^2\Delta M_2 \tag{4}$$

where τ_c denotes the correlation time, γ the magnetogyric ratio, ω_0 the Larmor frequency, ΔM_2 the second-moment reduction due to reorientation and C the relaxation constant.

Taking into account the experimental value $\Delta M_2 = 7\ G^2$, we can calculate the relaxation constant as $C = 3.34 \times 10^9\ s^{-2}$.

From the minimum of T_1 at 326 K for 60 MHz we can calculate $C = \omega_0/(1.425 \times T_{1min}) = 2.54 \times 10^9\ s^{-2}$.

The agreement of the relaxation constants determined from ΔM_2 and the T_1 minimum shows that the same kind of molecular motion is responsible for the observed T_1 relaxation and the reduction of the second moment.

Assuming that the motions responsible for the relaxation are thermally activated and using formulae (3) and (4), activation parameters for ring puckering were obtained by fitting experimental T_1 data. The obtained values are collected in table 3. The result of the fit is shown by the solid line in figure 6.

Table 3. The activation parameters in the high-temperature phase.

Type of motion	Activation energy (kJ mol^{-1})	τ_0 (s)	C (s^{-2})
ring puckering	26.1	0.87×10^{-13}	2.67×10^{9}

3.3.2. Low-temperature phase. It is evident that in the low-temperature phase the activation energy of ring puckering is higher. Moreover, a small change in the second-moment value occurring throughout the wide temperature range 120–223 K indicates that molecular motion in this phase can occur between potential energy minima of different value. In view of that, two different possible models of reorientation in the low-temperature phase have been considered:

model I assuming reorientation between two equivalent potential energy minima, and

model II assuming reorientation between two inequivalent potential energy minima.

For model I the activation parameters were obtained as the best fit to the experimental values of relaxation times T_1 for frequencies of 25 and 60 MHz, using equations (3) and (4), similarly as in the case of the high-temperature phase.

For model II we applied a similar procedure but on the basis of the formulae proposed in [8]:

$$(1/T_1)^{RP} = C[4a/(1+a)^2][\tau_c/(1+\omega_0^2\tau_c^2) + 4\tau_c/(1+4\omega_0^2\tau_c^2)] \tag{5}$$

and

$$\tau_c = [a/(1+a)K]\exp(E_a/RT) \tag{6}$$

$$a = \exp(\Delta/RT) \tag{7}$$

where Δ is the difference between the potential energy minima, E_a is the difference between the potential energy maximum and the higher value of the minima, and K is a frequency factor independent of temperature.

Table 4. The activation parameters in the low-temperature phase.

	C (s^2)	τ_0 (s)	K (s^{-1})	E_a (kJ mol^{-1})	Δ (kJ mol^{-1})
model I	2.26×10^{9}	0.57×10^{-15}	—	36.1	—
model II	2.09×10^{9}	—	6.27×10^{14}	32.3	4.2

The activation parameters obtained for the two models of reorientation are collected in table 4.

As a criterion for choosing the most appropriate model we used the temperature dependence of the second moment determined by the above obtained activation parameters. The calculations were performed using the following formula [9]:

$$M_2 = M_2^R\{1 - 3a/(1+a)^2 + [3a/(1+a)^2](2/\pi)\tan^{-1}(\gamma M_2^{-1/2}\tau_c)\} \tag{8}$$

where M_2^R is the second moment of a rigid lattice.

The results of both models are presented in figure 5, which shows that the dependence $M_2(T)$ based on model II is much closer to the experimental one, particularly up to 220 K, than that based on model I.

The fact that for the higher-temperature phase the measured second-moment values are lower than the estimated ones under the assumption of a constant Δ means that Δ could

be temperature-dependent. Moreover, by fitting the theoretical M_2 values to the measured ones we could determine the value of Δ at a given temperature. At a temperature very close to the phase transition, the parameter Δ takes a value of RT, similarly as for pyridinium nitrate [9].

For the relaxation process responsible for the T_1 shortening below 172 K the following activation parameters were obtained using equations (3) and (4):

$C = 9.7 \times 10^9\ s^{-2}$ $\quad \tau_0 = 3.1 \times 10^{-13}\ s$ $\quad$ and $\quad E_a = 2.2\ kJ\ mol^{-1}$.

The above value of the relaxation constant C is close to the value calculated for an isolated methyl group, which is $8.05 \times 10^9\ s^{-2}$ taking the H–H non-bonding distance as 1.78 Å. Therefore we can conclude that this process of relaxation is related to the reorientation of the methyl group, which has been additionally confirmed by the theoretically calculated second-moment values.

The final result of the fit between the theoretical and experimental temperature dependence of T_1 following from the proposed model of molecular reorientation in the low-temperature phase (first two terms in equation (2)) is shown in figure 6 by the solid line.

3.4. Dielectric measurements

The dielectric permittivity measurements are shown in figure 7 for some frequencies of measuring electric field. The dispersion of the real part of the dielectric permittivity is noticeable; however, there is no relaxation step at T_c. The permittivity value starts to decrease at room temperature and decreases more rapidly around T_c. For temperatures from 200 K down to 77 K the permittivity is almost temperature-independent. It is reasonable to assume that the decrease of permittivity is caused by the flipping process of the C(5) and C(4) methylene groups in the MCHD molecular ring, and although these vibrations mainly proceed along the c axis some components parallel to the (a, b) plane can appear. It is also possible that the vibrations of the molecule as a whole, which are coupled with the large-amplitude vibrations of C(4) and C(5), also contribute to the observed changes in the permittivity. For higher frequencies we observed the $\tan\delta$ maximum which has a relaxational character. The relaxation time obtained from the equation $\omega\tau = 1$ can be described by the Arrhenius equation:

$$\tau = \tau_0 \exp(E_a/RT). \tag{9}$$

The plot in logarithmic scale of τ versus $1/T$ is shown in figure 8. The activation energy $E_a = 31 \mp 6\ kJ\ mol^{-1}$ is compatible with the high-temperature phase activation energy obtained from our NMR measurements. We can conclude that the ring-puckering process observed in NMR measurements is actually seen in the dielectric permittivity experiment. The dielectric measurements confirm also the second-order character of the phase transition in MCHD at 243 K because of the absence of any step at T_c which also rather excludes a ferroelectric phase transition. The change of the dielectric permittivity from 4.8 at room temperature to 3.5 below 200 K discloses the freezing of the electric dipole moment of MCHD at temperatures below T_c.

3.5. Proton transfer

A possible type of molecular transformation in the MCHD structure is a transfer of the enolic proton in the hydrogen bond: from the oxygen atom O(1) to O(2) of the neighbouring molecule at the equivalent position $0.5-x$, $y-0.5$, z. Such an H transfer has been observed

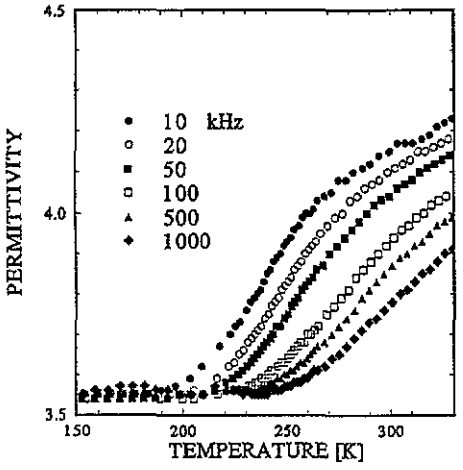

Figure 7. The real part of the dielectric permittivity of MCHD for various frequencies.

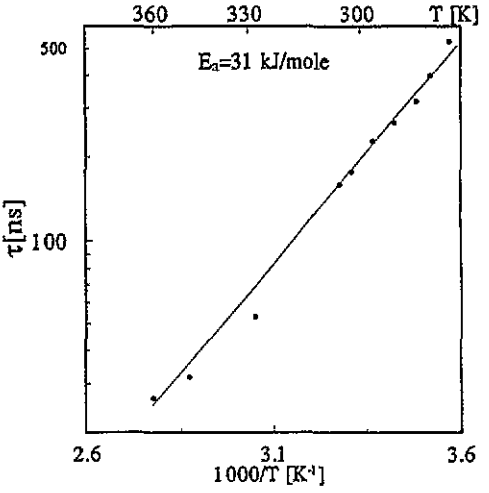

Figure 8. The activation energy of MCHD obtained from dielectric permittivity measurements.

at the phase transition in the CHD structure. It is accompanied by a transformation of the alternated π-electron bond system of molecules: from HO–C=C–C=O to O=C–C=C=OH.

Most recently it has been shown that the H-atom position in the hydrogen bond is coupled with the orientation of the hydrogen-bonded groups [10]. This coupling also applies to the structures of ferroelectric crystals, so-called KDP-type ferroelectrics, where spontaneous polarization is connected with ordering of protons in the hydrogen bonds. It has been demonstrated that the magnitudes of these displacements can be correlated with T_c of the ferroelectric–paraelectric phase transitions [11, 12]. This interdependence implies that one can assess the likeliness of a proton transfer by considering displacement of a molecule or ion from its position required by the structure with disordered protons [13]. In the MCHD structure this displacement can be measured as the inclination of the MCHD molecule, or the line drawn through its two oxygen atoms, to the direction of the hydrogen-bonded chain. This inclination angle (in degrees) in MCHD at room temperature is $\rho = 7.95(1)°$, and is larger than that in CHD of 3.38(2)° at room temperature, or of 7.20(1)° below the phase transition at 273 K. It is *much higher than the displacements observed in KDP-type* ferroelectrics [12]; thus disordering of the proton is highly unlikely.

Another possibility of molecular movements involving proton transfer is soliton waves proceeding along the hydrogen-bonded chains. Such a transfer, however, would have to be coupled with reorientations of the molecules by angle 2ρ, i.e. by 15.90°, which would be easily detected by measurements of NMR second moment M_2. Based on the NMR calculations it can be determined that such reorientations do not take place either above or below 243 K. This behaviour is different from that of CHD crystals, where molecular reorientations coupled with proton transfers and flipping of the methylene C(5)H_2 group to the other side of the ring plane where observed down to about 200 K, that is about 90 K below the phase transition. The M_2 measurements and calculations indicate that in MCHD neither of these movements are present at low temperatures; only ring puckering reorientation is present in the high-temperature phase. On the other hand, the dielectric permittivity measurements seem to indicate that no ferroelectric ordering of the

methylene groups takes place in the MCHD structure below T_c. The main contribution to the dipole moment of the MCHD molecule comes from the O=C–C=C–OH moiety while only very small or net atomic charges are present in methylene groups $C(4)H_2$ and $C(5)H_2$ of neighbouring molecules and the coupling is too weak to create ferroelectricity. Another possibility is that their positions are correlated below T_c; however the interaction of the methylene group with an external electric field is too weak to be detected in our experiments. Clearly further studies are required in order to conclude whether the MCHD structure undergoes a ferroelectric phase transition.

4. Conclusions

The entropy of the phase transition in MCHD was estimated as 5.7 J mol^{-1} K^{-1} from DSC measurements and is very close to the theoretical value $R \ln 2$ for an order–disorder transition. The disorder in the high-temperature phase is caused by C(4) and C(5) methylene groups of the molecular ring. The tail on the $C_p(T)$ curve below $T_c = 243$ K and the lack of hysteresis confirm the continuous type of the phase transition.

Two types of molecular motions were considered in NMR experiments: methyl group reorientation and methylene group conformational motion of the cyclohexene ring (ring puckering). The activation parameters of ring-puckering motions, which are connected with disorder of the molecular ring, have been estimated and two models of reorientation in the low-temperature phase were considered: (I) reorientation between two equivalent potential minima, and (II) reorientation between two non-equivalent potential energy minima. Model II appears to describe better the experimental results.

The dielectric measurements did not confirm the possibility of paraelectric–ferroelectric phase transition at T_c in MCHD because of the lack of a step on the temperature dependence of the permittivity. The steady decrease of the permittivity with decreasing temperature and dispersion is connected with the ordering process of the molecular ring around T_c. The activation energy of the molecular motion was estimated.

From the Brillouin scattering measurements we estimated the elastic constant tensor of MCHD. The large value of elastic anisotropy follows from the fact that the oxygen atoms along the b axis are involved in hydrogen bonding along this average direction. The elastic force constant $k_c = 5.4$ N m^{-1} is very typical of van der Waals interaction in organic crystals, but the high value of $k_b = 18$ N m^{-1} is caused by hydrogen bonding along the molecular chain. There is no discontinuity on the Brillouin frequency shift curve versus temperature, which confirms the continuous character of the phase transition.

Acknowledgments

The authors wish to dedicate this work to Professor Zdzisław Pająk on the occasion of his 70th birthday. Thanks are also due to Dr A Kozak for assistance in calculations. This work was supported by the Project 2 P30219304.

References

[1] Katrusiak A 1993 *J. Crystallogr. Spectrosc. Res.* **23** 367
[2] Katrusiak A 1990 *Acta Crystallogr.* B **47** 398
[3] Szafrański M, Czarnecki P, Katrusiak A and Habryło S 1992 *Solid State Commun.* **82** 277
[4] Pająk Z, Latanowicz L and Katrusiak A 1992 *Phys. Status Solidi* a **130** 421
[5] Mock R, Hillebrands B and Sandercock R J 1987 *J. Phys. E: Sci. Instrum.* **20** 656

[6] Van Vleck J H 1948 *Phys. Rev.* **74** 1168
[7] Blombergen N, Purcell E M and Pound R V 1949 *Phys. Rev.* **73** 679
[8] Look D C and Lowe I J 1966 *J. Chem. Phys.* **44** 2995
[9] Kozak A, Grottel M, Wąsicki J and Pająk Z 1994 *Phys. Status Solidi* a **143** 65
[10] Katrusiak A 1992 *J. Mol. Struct.* **269** 329
[11] Katrusiak A 1993 *Phys. Rev.* B **48** 2992
[12] Katrusiak A 1995 *Phys. Rev.* B **51** 589
[13] Katrusiak A 1994 *Correlations, Transformations and Interactions in Organic Crystal Chemistry* ed D W Jones and A Katrusiak (Oxford: Oxford University Press) pp 93–113